



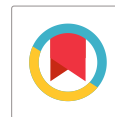
# Affinity of Cytotoxic Copper(II) Complex to Bovine Serum Albumin

S. Sangeetha, M. Murali\*

Department of Chemistry, National College (Autonomous), Tiruchirappalli, TN, India

Received: 22.03.2016 Accepted: 18.08.2016 Published: 30-09-2016

\*ma66mu@gmail.com



## ABSTRACT

The interaction of water soluble copper(II) complex,  $[\text{Cu}(\text{dipica})(\text{CH}_3\text{COO})]\text{ClO}_4$  (**1**), where dipica is di-(2-picolyl)amine, as in vitro cytotoxic agent, with bovine serum albumin (BSA) has been studied by fluorescence, UV-Vis absorption and circular dichroism (CD) spectroscopic techniques at pH 7.4. The quenching constants and binding parameters such as binding constants and number of binding sites were determined by fluorescence quenching method. The obtained results proved that the fluorescence quenching of BSA by **1** was a result of the formation of a non-fluorescent BSA-**1** system with the binding constants of  $1.81 \times 10^5 \text{ M}^{-1}$  and  $2.10 \times 10^5 \text{ M}^{-1}$  at 300 K and 310 K respectively. The calculated thermodynamic parameters ( $\Delta G^\circ$ ,  $\Delta H^\circ$  and  $\Delta S^\circ$ ) confirmed that the binding reaction is mainly entropy-driven and hydrophobic forces played major role in the reaction. The distance,  $r$ , between the donor (BSA) and acceptor (**1**) was obtained according to the Förster theory of nonradiative energy transfer. On the other hand, structural analysis indicates that binding of **1** resulting in a higher change in the local polarity around tryptophan rather than tyrosine residues of BSA as revealed by synchronous fluorescence spectra and a decrease in  $\alpha$ -helix as revealed by the far-UV CD spectra.

**Keywords:** BSA interaction; Copper(II) complex; Cytotoxicity; Hydrophobic forces; Static quenching.

## 1. INTRODUCTION

Metal-based antitumor drugs such as cisplatin, carboplatin and oxaliplatin are successfully used in the treatment of many cancer types with a high social incidence. However, there are problems associated with their use due to serious toxicity, severe side effects and promoted drug resistance (Galanski *et al.* 2005). The unsolved problems in platinum-based anticancer therapy has stimulated increased research efforts in the search for novel molecules or novel DNA-targeting anticancer agents which are capable of interacting with nucleic acids and even triggering apoptosis in cancer cells (Yuan *et al.* 2009). Copper complexes could be good candidates owing to the fact that copper is recognized as a bioessential element for human (Waddell *et al.* 1929) and characterization of its role for biological applications and potential pharmacological activity is extensively addressed in the development of copper-based drugs (Chen *et al.* 2011).

Serum albumin is the most abundant protein in plasma ( $\sim 40 \text{ mg mL}^{-1}$ ,  $0.6 \text{ mM}$ ; Keppler *et al.* 1993), and is responsible for the transport and distribution of a wide variety of endogenous and exogenous substances (Kragh-Hansen *et al.* 1981), including fatty acids, hormones, metal ions and drugs. Many drugs and other bioactive molecules can bind reversibly to serum albumins. Binding studies are important, because only the unbound drug is pharmacologically active (Arnell *et al.* 2006).

Among serum albumins, bovine serum albumin (BSA) is an appropriate protein model for studying the interaction between serum albumins and drugs because of its medically important, unusual ligand-binding properties, ease of availability, low cost and structural homology with human serum albumin (HSA; Hu *et al.* 2005). BSA is composed of three linearly arranged, structurally homologous subdomains (A and B). It has two tryptophan residues that possess intrinsic domains (I-III) and each domain in turn is the product of two fluorescence: Trp-134 is located on the surface of subdomain IB, and Trp-212 is located within the hydrophobic binding pocket of subdomain IIA (Peters, 1985). The binding sites of BSA for endogenous and exogenous ligands may be in these domains and the principal regions of drugs binding sites of albumin are often located in hydrophobic cavities in subdomains IIA and IIIA. So-called sites I and II are located in subdomains IIA and IIIA of albumin respectively.

Whether one compound can be used as drugs or not, it is important to test various chemical and biochemical properties in the identification of the most active drugs. It is well known that the interaction between drugs and albumin in the blood affects the distribution, free concentration and the metabolism of the drug. The interaction can also influence the drug stability and toxicity during the chemotherapy process. The number of

drug binding sites and their respective binding affinities affect the concentration of the free/active compound in the plasma. Strong binding to albumin can reduce the efficacy, distribution and clearance of the drug, and as such, weaker binding may be more useful for drug transport (Curry *et al.* 1998). Therefore, the interaction between serum albumins and drugs not only provide useful information on the structural features that determine the therapeutic effectiveness of drugs, but is also crucial to study the pharmacological response of drugs and design of dosage forms. In recent years, many studies on the interaction of serum albumin with organic molecule using fluorescence, absorption, synchronous fluorescence and circular dichroism spectra are reported. However, the studies of the interaction of serum albumin and metal complex are infrequent.

Very recently, a water soluble copper(II) complex (Sangeetha *et al.* 2015) [Cu(dipica)(CH<sub>3</sub>COO)]ClO<sub>4</sub> 1, where dipica is di-(2-picolyl)amine, has been synthesized. It has been involved in groove binding mode of interaction with calf thymus (CT) DNA. Interestingly, it has a profound efficiency to cleave pUC 19 DNA at acidic pH. Also, it showed significant *in vitro* cytotoxicity (IC<sub>50</sub>, 55 μM) against human cervical carcinoma cell line (HeLa) and notably, it was non-toxic to healthy cells. Therefore, in the present work, to further explore and expand our understanding of transport and distribution through the reversible binding of 1 to the blood carrier protein BSA, we continued to investigate the binding properties of 1 to BSA at physiological pH and temperatures of 27 °C (room temperature) and 37 °C (physiologic temperature). Using different spectroscopic methods, the binding information, including quenching mechanism, binding parameters, thermodynamic parameters, binding mode, intermolecular distances and conformational changes were investigated.

## 2. EXPERIMENTAL METHODS

### 2.1 Materials and Methods

BSA was purchased from Sigma Aldrich and used without further purification. The stock solution of protein (1.0 × 10<sup>-4</sup> mol L<sup>-1</sup>) was prepared by dissolving the solid BSA in 0.05 M phosphate buffer at pH 7.4 and stored at 0-4 °C in the dark for about a week and then diluted to 1.0 × 10<sup>-6</sup> mol L<sup>-1</sup> using phosphate buffer (pH 7.4, 0.05 M) when used. The concentration of BSA was determined from optical density measurements, using the value of molar absorptivity of ε<sub>280</sub> = 44720 M<sup>-1</sup> cm<sup>-1</sup>. The copper (II) complex (1) was synthesized on the basis of a literature method (Sangeetha *et al.* 2015). A stock solution of 1 (2.0 × 10<sup>-3</sup> mol L<sup>-1</sup>) was prepared in water. All other chemicals were of analytical reagent grade and doubly distilled water was used throughout. All experiments were done in 0.05 M phosphate buffer (pH 7.4).

All fluorescence measurements were performed using a Shimadzu RF-5301PC spectrofluorophotometer equipped with a thermostatic bath and a 10 mm quartz cuvette. Fluorescence emission spectra were recorded at two different temperatures (27 and 37 °C). UV-Vis absorption spectra were recorded using Perkin-Elmer Lambda 35 UV-Visible spectrophotometer. Circular Dichroic spectra of BSA were obtained by using JASCO J-716 spectropolarimeter. The pH was potentiometrically measured using a Elico LI 120 pH meter equipped with a combined glass electrode.

### 2.2 Procedures

The UV-Visible absorption spectra of 1.0 μM free BSA as well as BSA/copper(II) complex (equal molar ratio) in 0.5 M phosphate buffer of pH 7.4 were recorded from 200-500 nm.

Quantitative analyses of the interaction between copper (II) complex and BSA were performed by fluorimetric titration (0.5 M phosphate buffer, pH 7.4). A 3.0 ml portion of an aqueous solution of BSA (1.0 × 10<sup>-6</sup> mol L<sup>-1</sup>) was titrated by successive additions of complex (to give a final concentration of 8.0 × 10<sup>-6</sup> mol L<sup>-1</sup>). Titrations were done manually by using an Eppendorf micro pipette. For every addition, the mixture solution was shaken and allowed to stand for 20 min at the corresponding temperature (300 and 310 K), and then the fluorescence intensities were measured with an excitation wavelength of 280 nm and emission wavelengths in the interval 290-500 nm. No correction for the inner filter effect was applied since copper(II) complex represented very low absorbance (less than 0.1) at excitation and emission wavelengths. The excitation and emission slit width (each 5.0 nm), scan rate (fast) were constantly maintained for all the experiments. In the meantime, the synchronous fluorescence intensity of the mixed solution was measured at Δλ = 15 nm and Δλ = 60 nm, respectively. In synchronous fluorescence spectroscopy, according to Miller (Miller, 1979), distinction of the difference between excitation wavelength and emission wavelength (Δλ = λ<sub>em</sub>-λ<sub>ex</sub>) reflects the spectra of a different nature of chromophores, with large Δλ values such as 60 nm, the synchronous fluorescence of BSA is characteristic of tryptophan residue and with small Δλ values such as 15 nm is characteristic of tyrosine (Tang *et al.* 2006).

The far-UV CD measurements of BSA (1.0 μM) in the absence and presence of copper(II) complex (1:0.1, 1:0.2, 1:0.3) were recorded from 200 to 260 nm in 0.5 M phosphate buffer (pH 7.4) at room temperature.

## 3. RESULTS & DISCUSSION

### 3.1 Fluorescence Quenching Studies

Quantitative analysis of binding of chemical compounds to BSA can be detected by examining fluorescence spectra. Generally, the fluorescence of a

protein is caused by three intrinsic characteristics of the protein, namely tryptophan (Trp), tyrosine (Tyr) and phenyl alanine (Phe) residues. Actually, the intrinsic fluorescence of many proteins is mainly contributed by tryptophan alone. Fluorescence quenching refers to any process which causes a decrease of the fluorescence intensity from a fluorophore due to a variety of molecular interactions. These include excited-state reactions, molecular rearrangements, energy transfer ground-state complex formation and collisional quenching. Thus, the interaction of complex 1 with BSA was monitored by studying the quenching fluorescence of BSA with increasing concentration of 1 at 300 and 310 K in the

wavelength range 290-500 nm by exciting the BSA at 280 nm. The effect of 1 on the BSA fluorescence intensity is shown in fig. 1. The concentration of BSA was stabilized at  $1.0 \times 10^{-6} \text{ mol L}^{-1}$  and the concentration of 1 varied from 0.2 to  $8.0 \times 10^{-6} \text{ mol L}^{-1}$ . The fluorescence intensity of BSA decreased regularly with increasing concentration of 1 and a decrease up to 80.6% (300 K) and 89.1% (310 K) of the initial fluorescence intensity of BSA at 340 nm which is accompanied by a blue shift of 3-4 nm. The observed blue shift is mainly due to the fact that the active site in a protein is buried in a hydrophobic environment indicating a definite interaction of 1 with BSA protein.

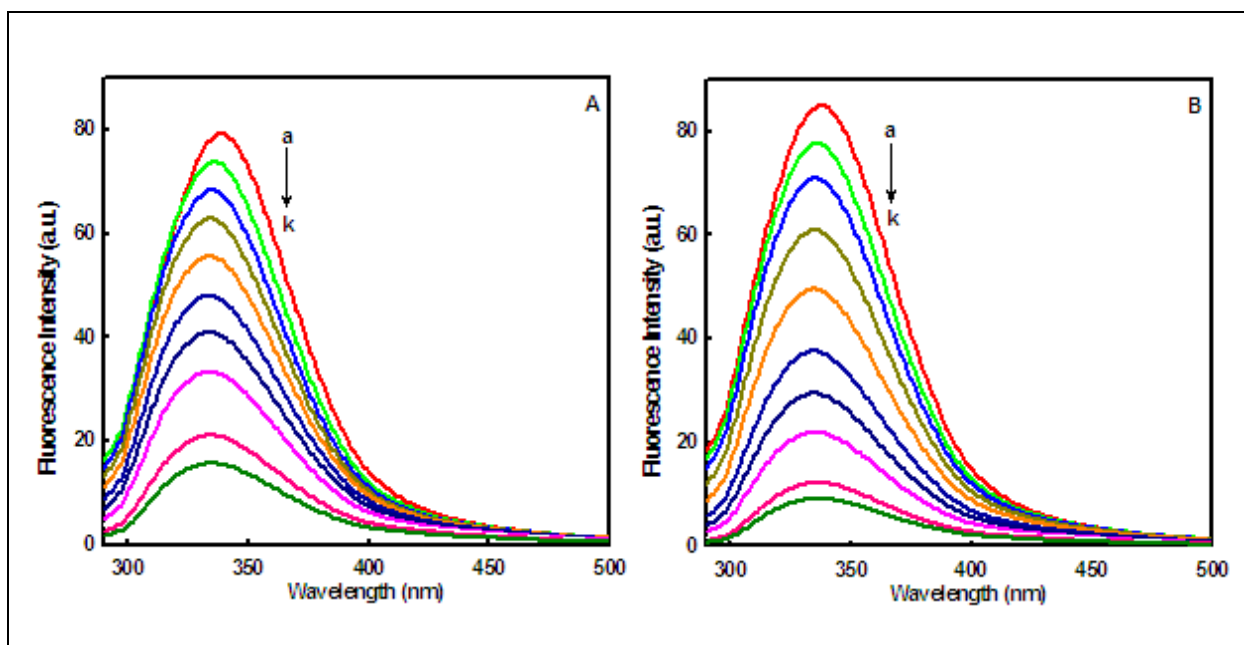


Fig. 1: Changes in the fluorescence spectra of BSA through the titration with complex 1 at 300 K (left, A) and 310 K (right, B). The concentration of BSA is  $1 \times 10^{-6} \text{ mol L}^{-1}$ , and the concentration of 1 was varied from (a) 0.0 to (k)  $8.0 \times 10^{-6} \text{ mol L}^{-1}$ ; pH 7.4 and  $\lambda_{\text{ex}} 280 \text{ nm}$

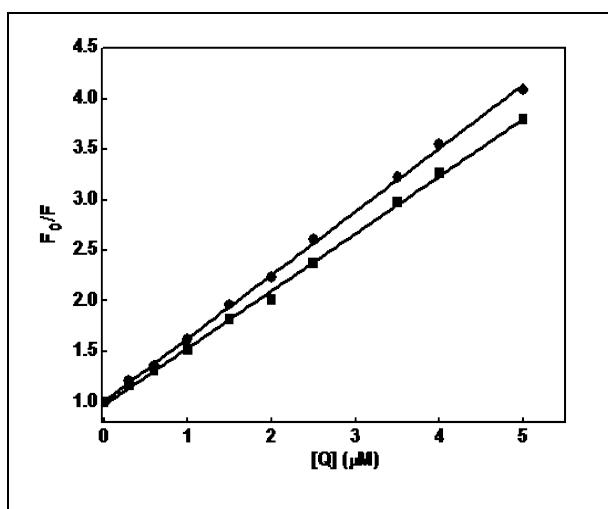


Fig. 2: The Stern-Volmer plots of BSA on different temperature for 1.  $\lambda_{\text{ex}} = 280 \text{ nm}$  (300K (■) and 310K (●)); pH = 7.4

Quenching can occur by different mechanisms, which are usually classified as dynamic and static quenching. Dynamic quenching refers to a process in which the fluorophore come into contact during the transient existence of the excited state. Static quenching refers to fluorophore-quencher complex formation. In general, dynamic and static quenching can be distinguished by their differing dependence on temperature and excited state lifetime. In both the cases, the change in fluorescence intensity is related to the concentration and nature of the quencher. Therefore, the quenched fluorophore can serve as an indicator for quenching agent. The mechanism of fluorescence quenching can be described by the following Stern-Volmer equation (Lakowicz, 2006):

$$F_0/F = 1 + K_{SV}[Q] = 1 + k_q\tau_0[Q]$$

Where  $F_0$  and  $F$  are the steady-state fluorescence intensities in the absence and presence of quencher, respectively,  $K_{SV}$  is the Stern-Volmer quenching constant,  $[Q]$  is the total concentration of quencher,  $k_q$  is the bimolecular quenching constant and  $\tau_0$  is the average lifetime of protein in the absence of quencher and its value is  $10^{-8}$  s (Lakowicz *et al.* 1973). Fig. 2 displays the Stern-Volmer plots of the quenching of BSA fluorescence by 1 at different temperatures. As seen, the plot of  $F_0/F$  for BSA *versus*  $[1]$ , ranging from 0.2 to  $8.0 \times 10^{-6}$  mol L $^{-1}$  at 300 and 310 K are both linear. As it is known, linear Stern-Volmer plots represent a single quenching mechanism; either static or dynamic occurs at these concentrations (Eftink *et al.* 1981).

The dynamic and static quenching can be differentiated by their temperature dependence. Dynamic quenching depends upon diffusion. Since higher temperatures result in higher diffusion coefficients, the bimolecular quenching constants are expected to increase with increasing temperature. In contrast, in static quenching, increased temperature is likely to decrease the fluorophore-quencher stability constant resulting in lower values of static quenching constants (Chen *et al.* 1990). The results in Table 1 show that  $K_{SV}$  increases with rising temperature, indicating that the fluorescence quenching of BSA by 1 is likely to occur via a dynamic quenching mechanism (Chen *et al.* 2008). In addition, according to  $K_q = K_{SV}/\tau_0$  the quenching rate constant  $K_q$  can be calculated. The obtained bimolecular quenching constant  $K_q$  for 1 is on the order of  $10^{13}$  L mol $^{-1}$  s $^{-1}$  (Table 1), which is 1000- fold higher than the maximum scatter collision- quenching (Zhao *et al.* 2010). This indicates that the quenching is not initiated by the dynamic collision, but by a static one due to the formation of BSA-1 complex. Thus, the present complex can be stored and moved by the protein in the body (Cheng *et al.* 2008).

**Table 1. Quenching parameters of the interaction of [Cu(dipica)(CH<sub>3</sub>COO)]ClO<sub>4</sub> (1) with BSA at different temperatures<sup>a</sup>**

	T(K)	$10^{-5} K_{SV}$ (M $^{-1}$ ) $\pm$ SD	$k_q(10^{-13} M^{-1} s^{-1})$	R
BSA-1	300	$5.658 \pm 0.008$	5.658	0.9991
	310	$6.259 \pm 0.006$	6.259	0.9982

<sup>a</sup>R is the linear correlated coefficient.

Electronic absorption spectroscopy is a simple and effective technique to explore the structural changes of protein due to its interaction with a drug and consequently, detect the quenching process. For a dynamic quenching mechanism, the absorption spectra of the fluorescent substance is not changed, but only the excited state fluorescence molecule is influenced by quenchers. While, for static quenching, a new compound

is formed between the ground state of the fluorescent substance and quencher and, therefore, the absorption spectra of fluorescence substance would be considerably influenced (Eftink *et al.* 1981). The UV absorption of BSA in the presence and absence of 1 is shown in fig 3. The influence of the absorbance of 1 was eliminated by adding in the reference cell the solution of 1 of the same concentration as in the sample solution. As it can be seen from fig 3 (curve a), BSA possesses two absorption bands; a strong band around 210 nm represents the content of  $\alpha$ -helix in the protein and a weak band around 280 nm is due to the absorption of aromatic acid (Tyr, Phe and Trp) residues (Wang *et al.* 2013). A significant decrease in the 210 nm absorbance peak of BSA is observed upon addition of 1 to the BSA (fig. 3, curve b). This can be attributed to the induced perturbation of  $\alpha$ -helix of BSA by the interaction of the whole complex since the high binding constant of 1 confirms the significant role of the configuration of ligands around copper(II) (Samari *et al.* 2012). Furthermore, an obvious red shift of the absorption peak (from 210 nm to 221 nm) could also be observed with the addition of 1. Meanwhile, the absorption intensity of the 280 nm band is increased (fig. 3, curve b) by the addition of 1, indicating that more aromatic acid residues are extended into the aqueous environment. Trp-212 in BSA, which is originally buried in a hydrophobic pocket, is exposed to an aqueous environment to a certain degree (Wang *et al.* 2013). This result indicated that the microenvironment of three amino acid residues is altered and the tertiary structure of BSA is destroyed. These results show that the interaction between 1 and BSA is mainly a static quenching process. Thus, the copper(II) complex could circulate through the system and BSA serves as a depot of the complex in the body.

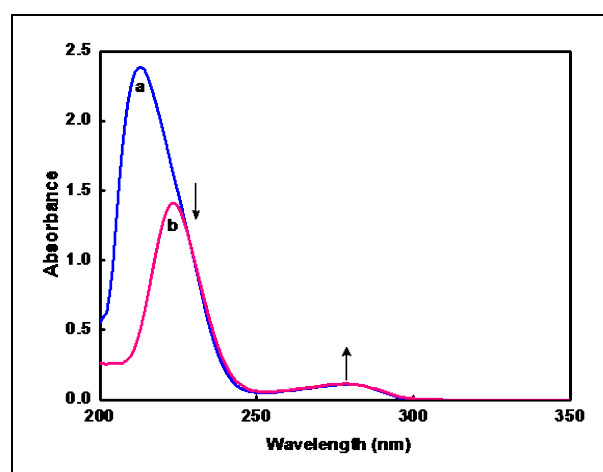


**Fig. 3: UV-Vis absorption spectra of BSA in the absence and presence of 1. (a) Absorption spectrum of BSA. (b) Absorption spectrum of BSA in the presence of 1 at the same concentration,  $[BSA] = [Cu \text{ complex}] = 3.5 \times 10^{-6}$  mol L $^{-1}$ . The absorbance of 1 is negligible in the spectral region shown.**



### 3.2 Binding Parameters

When small molecules bind independently to a set of equivalent sites on a macromolecule, the binding constant ( $K_b$ ) and the numbers of binding sites ( $n$ ) can be determined using the following equation (Divsalar *et al.* 2009):

$$\log[F_0 - F/F] = \log K_b + n \log [Q]$$

where  $K_b$  is the binding constant, reflecting the degree of interaction of BSA and 1, and  $n$  is the number of binding sites. Thus the plots of  $\log[(F_0 - F)/F]$  versus  $\log [Q]$  at 300 and 310 K give a straight line as depicted in fig 4. The values of  $n$  and  $K_b$  can be calculated from the slope and intercept of the linear plot respectively, and the results are listed in table 2. The binding constant increases with the rising temperature, which indicates that the capacity of 1 binding to BSA is enhanced endothermically at high temperature. The values of  $n$  equal to one indicate the existence of just a single binding site in BSA for 1. Of both tryptophans in BSA, Trp-212 is located within a hydrophobic binding pocket of the protein and Trp-134 is located on the surface of the albumin molecule. So, from the value of  $n$  it is proposed that the complex most likely binds to the hydrophobic pocket located in subdomain IIA (Sulkowska *et al.* 2003).

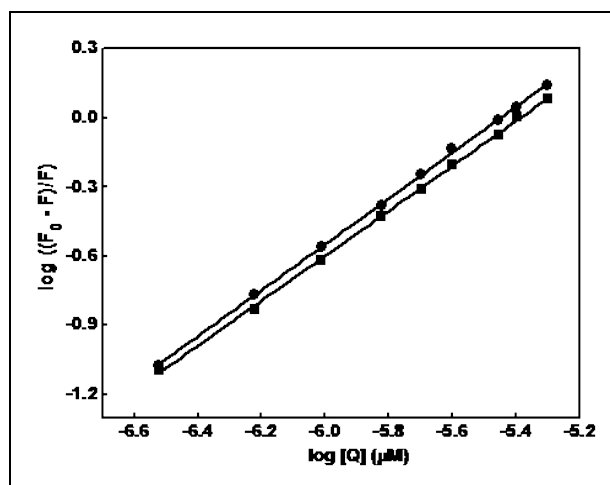


Fig. 4: Double-log plot of quenching effect of 1 on BSA fluorescence at 300K (■) and 310K (●).

Table 2. Binding parameters of the interaction of [Cu(dipica)(CH<sub>3</sub>COO)]ClO<sub>4</sub> (1) with BSA at different temperatures<sup>a</sup>

	T(K)	10 <sup>-5</sup> K <sub>b</sub> (M <sup>-1</sup> ) ± SD	n ± SD	R
BSA-1	300	1.805 ± 0.066	1.02 ± 0.01	0.9992
	310	2.103 ± 0.047	1.06 ± 0.01	0.9995

<sup>a</sup>R is the linear correlated coefficient.

### 3.3 Thermodynamic Parameters and Nature of the Binding Forces

Generally, the binding mode of a drug with biomolecules often contains hydrogen bonds, van der Waals forces, electrostatic force and hydrophobic interactions (Zhou *et al.* 2008). The enthalpy change can be regarded as a constant when the temperature does not vary significantly (Wang *et al.* 2010). The sign and magnitude of thermodynamic parameters such as  $\Delta H^\circ$  (enthalpy change),  $\Delta S^\circ$  (entropy change), and  $\Delta G^\circ$  (free energy change) of small molecules with proteins can account for the main forces of interaction. In order to elucidate the binding forces between 1 and BSA, the thermodynamic parameters were calculated from the Van't Hoff equations (Bi *et al.* 2009):

$$\ln(K_2/K_1) = (1/T_1 - 1/T_2) \Delta H^\circ/R$$

$$\Delta G^\circ = \Delta H^\circ - T\Delta S^\circ = -RT \ln K$$

where  $K$  is the equilibrium binding constant at the corresponding temperature,  $K_1$  and  $K_2$  are the binding constants at temperature  $T_1$  and  $T_2$ , respectively, and  $R$  is the gas constant. The calculated thermodynamic parameters are given in table 3.

Table 3. Relative thermodynamic parameters of BSA-[Cu(dipica)(CH<sub>3</sub>COO)]ClO<sub>4</sub>(1) system

	T(K)	$\Delta H^\circ$ (kJ mol <sup>-1</sup> )	$\Delta G^\circ$ (kJ mol <sup>-1</sup> )	$\Delta S^\circ$ (J mol <sup>-1</sup> K <sup>-1</sup> )
BSA-1	300	77.907	-33.037	110.386
	310		-34.399	111.217

Ross, Subramanian and Leckband (Ross *et al.* 1981; Leckband *et al.* 2000) have characterized the sign and magnitude of the thermodynamic parameters associated with particular kinds of interaction. From the thermodynamic standpoint, the positive values of both  $\Delta H^\circ$  and  $\Delta S^\circ$  implies a hydrophobic force; negative values for both  $\Delta H^\circ$  and  $\Delta S^\circ$  reflects the vander Waals force and hydrogen bond formation; and very low positive or negative  $\Delta H^\circ$  ( $\Delta H^\circ \approx 0$ ) and positive  $\Delta S^\circ$  values characterized by electrostatic force. From table 3 the negative sign for  $\Delta G^\circ$  indicates the spontaneity of the binding of 1 with BSA. The positive values obtained for both  $\Delta H^\circ$  and  $\Delta S^\circ$  indicate that a hydrophobic association is the major binding force and that the interaction is entropy driven process. In addition to hydrophobic interaction, a possible covalent bonding may be also considered. However, the value of  $\Delta H^\circ$  (78 kJ mol<sup>-1</sup>) obtained here is considerably below what would be expected for a covalent bond formation, which should be  $\geq 120$  kJ mol<sup>-1</sup> (Lunardi *et al.* 2003). Thus, the non-polar hydrophobic groups of the BSA may be responsible for

the main effect determining the binding of 1 and BSA. This, together with the number of binding sites, suggests that the binding site for 1 on BSA is primarily on the Trp-212 residues, which is located within a hydrophobic binding pocket of the protein.

### 3.4 Synchronous Fluorescence Spectroscopy

The synchronous fluorescence spectra can provide the information about the molecular environment in the vicinity of the chromophore molecules (Lloyd *et al.* 1977). The fluorescence of BSA comes from the tyrosine, tryptophan and phenylalanine residues. The spectrum of BSA was sensitive to the micro-environment of these chromophores and it allows non-intrusive measurements of protein in low concentration under physiological conditions (Jayabharathi *et al.* 2011). It has several advantages like spectral simplification, spectral bandwidth reduction, and avoidance of different perturbing effects (Cui *et al.* 2008). Therefore, the influence of metal complexes on the conformational changes of BSA was assessed by synchronous fluorescence spectra (Wu *et al.* 2006). Synchronous fluorescence spectra are obtained by simultaneous scanning of the excitation and emission monochromators. According to the theory of Miller (Miller, 1979), when  $\Delta\lambda$  between excitation wavelength and emission wavelength is set at 15 or 60 nm, the synchronous fluorescence offers characteristic information on the environment of tyrosine and tryptophan residues, respectively. The changes in maximum emission position correspond to the change in the polarity around the chromophore molecule. Thus, the environment of amino acid residues can be studied by measuring the shift in wavelength of emission maximum. The synchronous fluorescence spectra of BSA with various amounts of 1 were recorded at  $\Delta\lambda = 15$  nm and  $\Delta\lambda = 60$  nm (fig. 5). It can be seen from fig. 5 that the maximum emission wavelength of tyrosine and tryptophan residues represents a significant red shift (tyrosine: from 312 to 319; tryptophan, from 346 to 354 nm). The red shift of the maximum emission wavelength expresses the change in conformation of BSA; the polarity around the tyrosine and tryptophan residues is increased and the hydrophobicity is decreased (Zhang *et al.* 2007). In addition, synchronous fluorescence quenching ratios ( $R_{SFQ}$ ) are also calculated using the equation  $R_{SFQ} = 1 - F/F_0$  (fig. 6), in which, F and  $F_0$  are the synchronous fluorescence intensities of BSA in the presence and absence of 1, respectively. From the perspective of numerical calculation, at any compound concentration for the BSA-1 system, the  $R_{SFQ}$  for  $\Delta\lambda = 60$  nm (85.6%) is greater than the corresponding one for  $\Delta\lambda = 15$  nm (79.1%), indicating that the complex reached subdomain IIA, where the only one Trp-212 residue on BSA is located. There is a large hydrophobic cavity in subdomain IIA which many drugs could bind to them. Thus, the quenching of fluorescence intensities of

tryptophan residues are higher than that of tyrosine residues, suggesting that tryptophan residues contributed more to the quenching of intrinsic fluorescence. The above results indicated that the complex could bind BSA primarily in the hydrophobic cavity of subdomain IIA with higher binding affinity to form a stable BSA-1 system.

### 3.5 Energy Transfer from BSA to Copper(II) Complex

BSA has two tryptophan moieties (Trp-134 and Trp-212), located in subdomain IA and IIA respectively. The spectral studies suggested the formation of a BSA-1 system, leading to the conclusion that Trp-212 in BSA is the primary target of the complex, located in subdomain IIA. Fluorescence resonance energy transfer (FRET) is a non-destructive spectroscopic method that can monitor the proximity and relative angular orientation of fluorophores, the donor and acceptor fluorophores can be entirely separated or attached to the same macromolecule. A transfer of energy could take place through direct electro-dynamic interaction between the primarily excited molecule and its neighbours (Förster, 1948). The distance between the buried Trp-212 (as donor) and the interacted complex (as acceptor) was estimated by Förster's non-radiative energy transfer theory and the overlapping of the fluorescence spectrum of BSA with absorption spectrum of 1 was shown in fig. 7. According to Förster's non-radiative energy transfer theory, the energy transfer efficiency, E, is calculated using the following equation (Kang *et al.* 2004):

$$E = 1 - F/F_0 = R_0^6/R_0^6 + r^6$$

where r is the distance between the donor and acceptor and  $R_0$  is the critical distance when the transfer efficiency equals to 50% and the value of  $R_0$  is calculated by the following equation (Hof *et al.* 2005):

$$R_0 = 979(\kappa^2 n^{-4} \phi J)^{1/6} \text{ nm}$$

The term  $\kappa^2$  is the relative orientation of space of the transition dipole of the donor and acceptor (for a random orientation as in fluid,  $\kappa^2 = 2/3$ ), n is the refractive index of the medium in the wavelength range where spectral overlap is significant,  $\phi$  is the fluorescence quantum yield of the donor and overlap integral J expresses the extent of overlap between the donor emission and the acceptor absorption, which could be calculated by the following equation:

$$J = \int F(\lambda) \epsilon(\lambda) \lambda^4 d\lambda / \int F(\lambda) d\lambda$$

where  $F(\lambda)$  is the normalized donor emission spectrum in the range from  $\lambda$  to  $\lambda + \Delta\lambda$ , and  $\epsilon(\lambda)$  is the molar absorption coefficient of the acceptor at wave length  $\lambda$ . In the present case, we took  $n = 1.36$  and  $\phi = 0.15$  (Cyril

*et al.* 1961). According to the above equations, we obtain that  $J(\lambda) = 2.91 \times 10^{14} \text{ M}^{-1} \text{ cm}^3$ ,  $R_0 = 1.39 \text{ nm}$ ,  $E = 0.22$  and  $r = 4.97 \text{ nm}$ . The donor-to- acceptor distance is less than 8 nm, which indicates that the energy could transfer from BSA to 1 with high probability and the distance obtained by FRET with higher accuracy. Therefore, it reveals that the energy transfer quenches the fluorescence of BSA when 1 binds to BSA, which is a non-radiative energy transfer process.

### 3.6 Conformational Change of BSA in the Presence of copper(II) Complex

The absorption and emission spectral studies of copper(II) complex in the presence of BSA confirm the strong interaction between 1 and BSA. It is important to examine how the structure of BSA is affected in the presence of 1. When ligands bind to globular protein, the intramolecular forces responsible for maintaining the secondary and tertiary structures can be altered, resulting in a conformational change of the protein (Kragh-Hansen, 1981) The distinct fluorescence quenching along with blue shift observed in 1 in the presence of BSA suggest that the BSA-1 system has changed the micro-environment of BSA. Circular dichroism (CD) is one of the strong and sensitive spectroscopic techniques to monitor conformational changes of protein structure upon interaction with small molecules. BSA has a high percentage of  $\alpha$ -helical structure which shows a characteristic strong double minimum signal at 208 and 222 nm (fig. 8, curve a; Kelly *et al.* 2005). The reasonable explanation is that the negative peaks at 208 and 222 nm both contribute to  $n \rightarrow \pi^*$  transfer for the peptide bond of  $\alpha$ -helix. The copper(II) complex does not contribute to the CD signal in the range 200-260 nm, thus the observed CD is solely due to BSA. To ascertain the possible influence of 1 binding on the secondary structure of BSA, we have performed far-UV CD spectroscopy of BSA in the absence and presence ( $2.0$  to  $6.0 \times 10^{-7} \text{ M}$ ) of 1 (molar ratios of BSA in 1 were 1:0, 1:0.1, 1:0.2 and 1:0.3). The CD results are expressed in terms of the mean residue

ellipticity (MRE) in  $\text{deg cm}^2 \text{ dmol}^{-1}$  according to the following equation:

$$\text{MRE} = \theta_{\text{obs}} (\text{mdeg}) / 10nlC_p$$

where  $C_p$  is the molar concentrations of the protein,  $n$  the number of amino acid residues (583 for BSA) and  $l$  is the path length (0.1 cm). The  $\alpha$ -helical contents of free and combined BSA are calculated from MRE values at 208 nm using the following equation (Lu *et al.* 1987):

$$\alpha\text{-helix (\%)} = [-\text{MRE}_{208} - 4000 / 33000 - 4000] \times 100$$

where  $\text{MRE}_{208}$  is the observed MRE value at 208 nm, 4000 is the MRE of the  $\beta$ -form and random coil conformation cross at 208 nm and 33000 is the MRE value of a pure  $\alpha$ -helix at 208 nm. From the above equation, the  $\alpha$ -helicity in the secondary structure of BSA is determined. A set of far-UV CD spectra of BSA in the absence and presence of 1 at pH 7.4 and 300 K are given in fig. 8 and the inset shows the helicity of BSA *versus* [1] at 208 and 222 nm. The CD spectral data reveal the decrease in  $\alpha$ -helix structure of BSA (BSA to 1 molar ratio, % of  $\alpha$ -helix at 208 and 222 nm respectively: 1:0, 64.4 and 60.0%; 1:0.1, 62.2 and 57.8%; 1:0.2, 43.1 and 39.6%; 1:0.3, 32.7 and 27.4%), and is realized from the reduction in the intensity of double minima. According to the literature, far-UV (200-260 nm) CD spectra gave the quantitative information on the secondary structure and the near-UV (260-300 nm) CD spectra can infer the tertiary structure of BSA (Price, 2000). The CD spectra of BSA in the presence and absence of the 1 is observed to be similar in shape, that is, there is no additional signal in the near-UV region, change in the far-UV region indicates the secondary structure changes in BSA in the presence of copper(II) complex, which means that there is no change in the tertiary structure of BSA. Therefore, the structure of BSA is also predominantly of  $\alpha$ -helix. Hence, we can conclude that 1 causes a conformational change in BSA with the loss of  $\alpha$ -helicity.

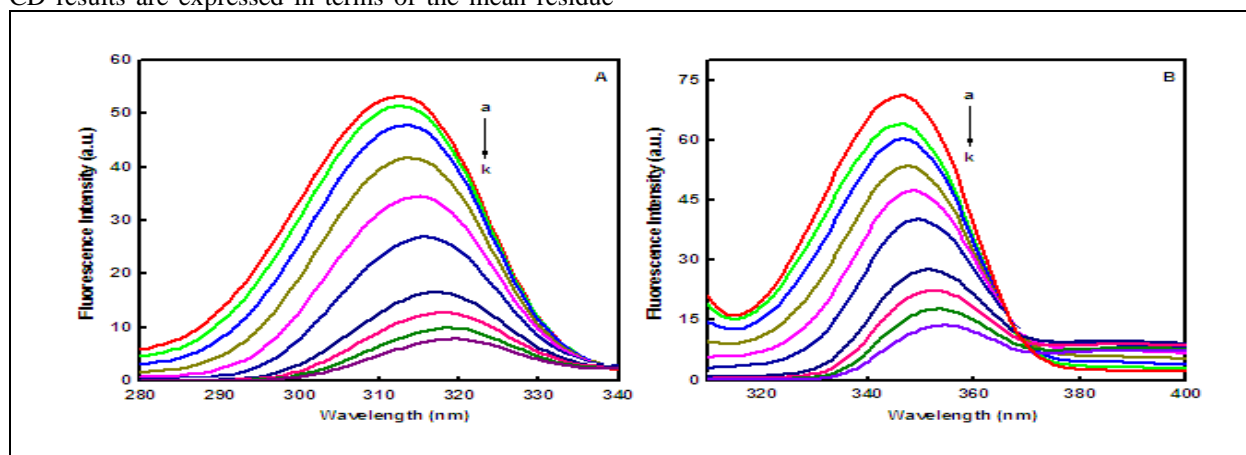


Fig. 5: Synchronous fluorescence spectra of BSA ( $1 \times 10^{-6} \text{ mol L}^{-1}$ ) upon addition of 1;  $\Delta\lambda = 15 \text{ nm}$  (A) and  $\Delta\lambda = 60 \text{ nm}$  (B). The concentration of 1 varied from (a) 0.0 to (k)  $8.0 \times 10^{-6} \text{ mol L}^{-1}$

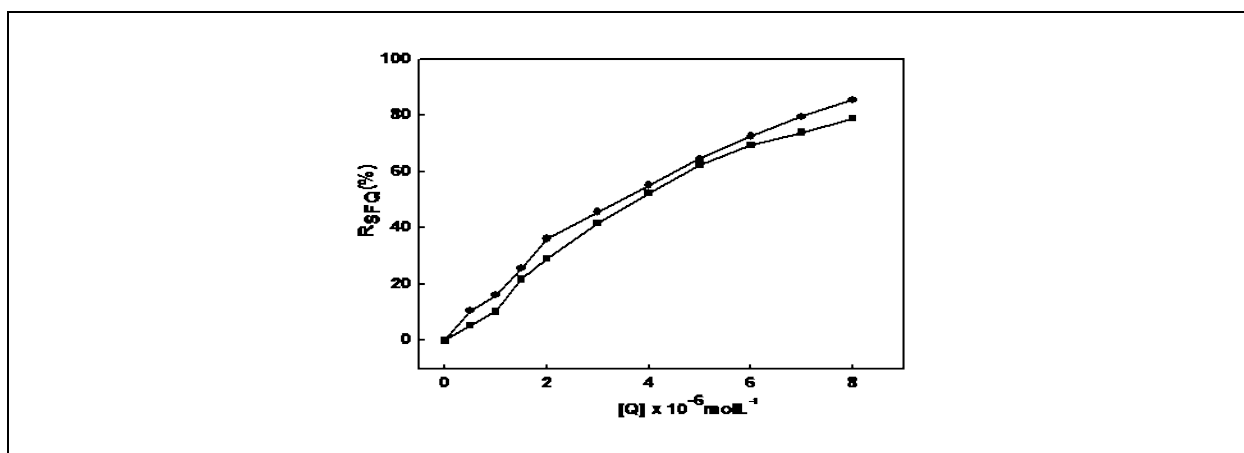


Fig. 6: Ratios of synchronous fluorescence quenching ( $R_{SFO}$ ) of BSA ( $1 \times 10^{-6} \text{ mol L}^{-1}$ ) upon addition of 1;  $\Delta\lambda = 15 \text{ nm}$  (■) and  $\Delta\lambda = 60 \text{ nm}$  (●). The concentration of 1 varied from (a) 0.0 to (k)  $8.0 \times 10^{-6} \text{ mol L}^{-1}$

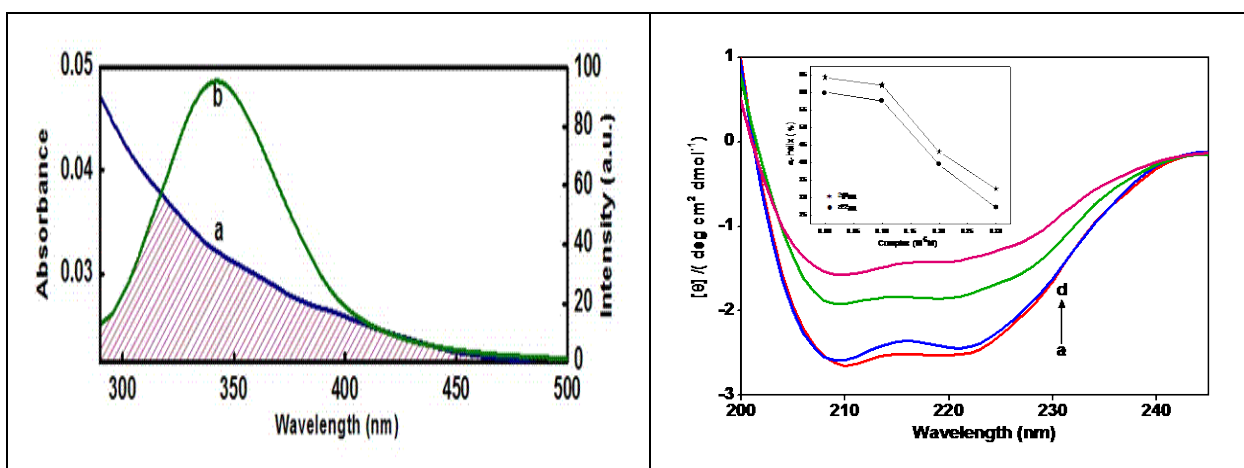


Fig. 7: Overlap of the fluorescence spectra of BSA and the absorption spectra of 1,  $[BSA] = [Cu \text{ complex}] = 1 \times 10^{-6} \text{ mol L}^{-1}$

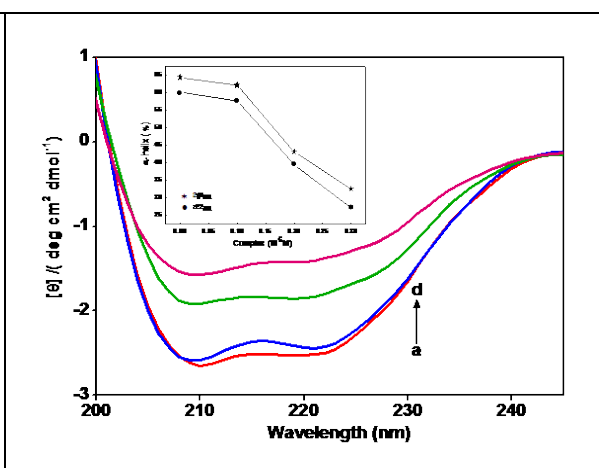


Fig. 8: The far-UV CD spectra for BSA in the absence (a) and presence (b-d) of 1.  $[BSA] = 1 \times 10^{-6} \text{ mol L}^{-1}$ . b-d:  $[1] = 1.0, 2.0, 3.0 \times 10^{-6} \text{ mol L}^{-1}$ . (Inset: Plot of the helicity of BSA versus the concentration of complex at 208 and 222 nm)

#### 4. CONCLUSIONS

The cytotoxic copper(II) complex binds to BSA with high affinity at a stoichiometric ratio of 1:1 and quenching of the fluorescence of BSA through a static quenching mechanism. The thermodynamic parameters,  $\Delta H^\circ$  and  $\Delta S^\circ$ , reveals that the BSA-1 system is stabilized by the hydrophobic forces. Furthermore, synchronous fluorescence data show that the BSA undergoes conformational changes upon binding to 1, where the complex is proposed to have the capability to bind with BSA at tryptophan residues. The distance between 1 and trptophan was estimated to be less than 8 nm, indicating that the energy transfer from BSA to 1 with high probability. This interaction causes a conformational change of the protein with the loss of  $\alpha$ -helix stability. Hence, the copper(II) complex could bind to BSA and be effectively transported and eliminated in the body. The

significant BSA binding and *in vitro* cytotoxicity results suggested that the present complex may be fit for the investigation of anticancer properties.

#### ACKNOWLEDGEMENTS

We are grateful to the DST-FIST programme of the National College (Autonomous), Tiruchirappalli. The authors thank Professor A. Ramu, School of Chemistry, and Madurai Kamaraj University for CD spectral measurements.

#### FUNDING

This research received no specific grant from any funding agency in the public, commercial, or not-for-profit sectors.



## CONFLICTS OF INTEREST

The authors declare that there is no conflict of interest.

## COPYRIGHT

This article is an open access article distributed under the terms and conditions of the Creative Commons Attribution (CC-BY) license (<http://creativecommons.org/licenses/by/4.0/>).



## REFERENCES

- Arnell, R., Ferraz, N. and Fornstedt, T., Analytical characterization of chiral drug-protein interactions: Comparison between the optical biosensor (Surface Plasmon Resonance) assay and the HPLC perturbation method, *Anal. Chem.*, 78, 1682-1689(2006).  
<https://doi.org/10.1021/ac0518021>
- Bi, S., Sun, Y., Qiao, C., Zhang, H. and Liu, C., Binding of several anti-tumor drugs to bovine serum albumin: Fluorescence study, *J. Lumin.*, 129, 541-547 (2009).  
<https://doi.org/10.1016/j.jlumin.2008.12.010>
- Cheng, Z. J. and Zhang, Y. T., Spectroscopic investigation on the interaction of salidroside with bovine serum albumin, *J. Mol. Struct.*, 889, 20-27 (2008).  
<https://doi.org/10.1016/j.molstruc.2008.01.013>
- Chen, G. Z., Haong, X. Z., Xu, J. C., Zhang, Z. Z. and Wang, Z. B., *The Methods of Fluorescence Analysis*, 2nd edn., pp. 2-112, Beijing Science Press (1990).
- Chen, J., Jiang, X. Y., Chen, X. Q. and Chen, Y., Effect of temperature on the metronidazole -BSA interaction: Multi-spectroscopic method, *J. Mol. Struct.*, 876, 121-126(2008).  
<https://doi.org/10.1016/j.molstruc.2007.06.011>
- Chen, Q. Y., Fu, H. J., Zhu, W. H., Qi, Y., Ma, Z. P., Zhao, K. D. and Gao, J., Interaction with DNA and different effect on the nucleus of cancer cells for copper(II) complexes of *N*-benzyl di(pyridylmethyl)amine, *Dalton Trans.*, 40, 4414-4420(2011).  
<https://doi.org/10.1039/C0DT01616K>
- Cui, F., Qin, L., Zhang, G., Liu, X., Yao, X. and Lei, B., A concise approach to 1,11-didechloro-6-methyl-4'-O-demethylrebeccamycin and its binding to human serum albumin: Fluorescence spectroscopy and molecular modeling method, *Bioorg. Med. Chem.*, 16, 7615- 7621 (2008).  
<https://doi.org/10.1016/j.bmc.2008.07.017>
- Curry, S., Mandelkow, H., Brick, P. and Franks, N., Crystal structure of human serum albumin complexed with fatty acid reveals an asymmetric distribution of binding sites, *Nat. Struct. Mol. Biol.*, 5, 827-835 (1998).  
<https://doi.org/10.1038/1869>
- Cyril, L., Earl, J. K. and Sperry, W. M., *Biochemist's Handbook*, p. 83, E and FN Epon Led, London (1961).
- Divsalar, A., Bagheri, M. J., Saboury, A. A., Mansoori-Torshizi, H. and Amani, M., Investigation on the interaction of newly designed anticancer Pd(II) complexes with different aliphatic tails and human serum albumin, *J. Phys. Chem. B*, 113, 14035-14042 (2009).  
<https://doi.org/10.1021/jp904822n>
- Eftink, M. R. and Ghiron, C. A., Fluorescence quenching studies with proteins, *Anal. Biochem.*, 114, 199-227 (1981).  
[https://doi.org/10.1016/0003-2697\(81\)90474-7](https://doi.org/10.1016/0003-2697(81)90474-7)
- Förster, T., Zwischenmolekulare energiewanderung und fluoreszenz, *Ann. Phys.*, 437, 55-75 (1948).  
<https://doi.org/10.1002/andp.19484370105>
- Galanski, M., Jakupec, M. A. and Keppler, B. K., Update of the preclinical situation of anticancer platinum complexes: Novel design strategies and innovative analytical approaches, *Curr. Med. Chem.*, 12, 2075-2094 (2005).  
<https://doi.org/10.2174/0929867054637626>
- Hof, M., Hutterer, R. and Fidler, V., *Fluorescence Spectroscopy in Biology*, Springer Science+Business Media, Berlin (2005).
- Hu, Y. J., Liu, Y., Jiang, W., Zhao, R. M. and Qu, S. S., Fluorometric investigation of the interaction of bovine serum albumin with surfactants and 6-mercaptopurine, *J. Photochem. Photobiol. B*, 80, 235-242 (2005).  
<https://doi.org/10.1016/j.jphotobiol.2005.04.005>

- Jayabharathi, J., Thanikachalam, V. and Venkatesh Perumal, M., Mechanistic investigation on binding interaction of bioactive imidazole with protein bovine serum albumin - A biophysical study, *Spectrochim. Acta Part A*, 79, 502-507 (2011).  
<https://doi.org/10.1016/j.saa.2011.03.020>
- Kang, J., Liu, Y., Xie, M., Li, S., Jiang, M. and Wang, Y.: Interactions of human serum albumin with chlorogenic acid and ferulic acid, *Biochim. Biophys. Acta*, 1674, 205-214 (2004).  
<https://doi.org/10.1016/j.bbagen.2004.06.021>
- Kelly, S. M., Jess, T. J. and Price, N. C., How to study proteins by circular dichroism, *Biochim. Biophys. Acta*, 1751, 119-139 (2005).  
<https://doi.org/10.1016/j.bbapap.2005.06.005>
- Keppeler, B. K., Lipponer, G., Stenzel, B. and Kranz, F., Metal complexes in cancer Chemotherapy, Verlag Chemie VCH, Weinheim (1993).  
<https://doi.org/10.1002/ange.19941060935>
- Kragh-Hansen, U., Molecular aspects of ligand binding to serum albumin, *Pharmacol. Rev.*, 33, 17-53 (1981).
- Lakowicz, J. R., Principles of Fluorescence Spectroscopy, 3rd edn., Springer Science+ Business Media, New York (2006).
- Lakowicz, J. R. and Weber, G., Quenching of fluorescence by oxygen. Probe for structural fluctuations in macromolecules, *Biochemistry*, 12, 4161-4170 (1973).  
<https://doi.org/10.1021/bi00745a020>
- Leckband, D. A.: Measuring the forces that control protein interactions, *Annu. Rev. Biophys. Biomol. Struct.*, 29, 1-26 (2000).  
<https://doi.org/10.1146/annurev.biophys.29.1.1>
- Lloyd, J. B. F., Evett, I. W., Prediction of peak wavelengths and intensities in synchronously excited fluorescence emission spectra, *Anal. Chem.*, 49, 1710-1715(1977).  
<https://doi.org/10.1021/ac50020a020>
- Lu, Z. X., Cui, T., Shi, Q. L., Application of Circular Dichroism and Optical Rotatory Dispersion in Molecular Biology, 1st edn., pp. 79-82, Science Press, Beijing (1987).
- Lunardi, C. N., Tedesco, A. C., Kurth, T. L., Brinn, I. M., The complex between 9-(*n*-decanyl)acridone and Bovine Serum Albumin. Part 2. What do fluorescence probes probe?, *Photochem. Photobiol. Sci.*, 2, 954-959 (2003).  
<https://doi.org/10.1039/B301789C>
- Miller, J. N., Recent advances in molecular luminescence analysis, *Proc. Analy. Div. Chem. Soc.*, 16, 203-208 (1979).  
<https://doi.org/10.3390/ijms140714185>
- Peters, T., Serum albumin, *Adv. Protein Chem.*, 37, 161-245 (1985).  
[https://doi.org/10.1016/S0065-3233\(08\)60065-0](https://doi.org/10.1016/S0065-3233(08)60065-0)
- Ross, P. D. and Subramanian, S., Thermodynamics of protein association reactions: forces contributing to stability, *Biochemistry*, 20, 3096-3102 (1981).  
<https://doi.org/10.1021/bi00514a017>
- Price, N. C., Conformational issues in the characterization of proteins, *Biotechnol. Appl. Biochem.*, 31, 29-40 (2000).  
<https://doi.org/10.1042/BA19990102>
- Samari, F., Hemmateenejad, B., Shamsipur, M., Rashidi, M. and Samouei, H., Affinity of two novel five-coordinated anticancer Pt(II) complexes to human and bovine serum albumins: A spectroscopic approach, *Inorg. Chem.*, 51, 3454-3464 (2012).  
<https://doi.org/10.1021/ic202141g>
- Sangeetha, S. and Murali, M., Water soluble copper(II) complex [Cu(dipica)(CH<sub>3</sub>COO)]ClO<sub>4</sub>: DNA binding, pH dependent DNA cleavage and Cytotoxicity, *Inorg. Chem. Commun.*, 59, 46-49 (2015).  
<https://doi.org/10.1016/j.inoche.2015.06.032>
- Sulkowska, A., Równicka, J., Bojko, B. and Sułkowski, W., Interaction of anticancer drugs with human and bovine serum albumin, *J. Mol. Struct.*, 651-653, 133-140 (2003).  
[https://doi.org/10.1016/S0022-2860\(02\)00642-7](https://doi.org/10.1016/S0022-2860(02)00642-7)
- Tang, J. H., Luan, F. and Chen, X. G., Binding analysis of glycyrrhetic acid to human serum albumin: fluorescence spectroscopy, FTIR, and molecular modeling, *Bioorg. Med. Chem.*, 14, 3210-3217 (2006).  
<https://doi.org/10.1016/j.bmc.2005.12.034>
- Waddell, J., Steenbock, H., Elvehjem, C. A., Hart, E. B., Donk, E. V., Further proof that the anemia produced on diets of whole milk and iron is due to a deficiency of copper, *J. Biol. Chem.*, 83, 251-260 (1929).
- Wang, T., Zhao, Z., Wei, B., Zhang, L. and Ji, L., Spectroscopic investigations on the binding of dibazol to bovine serum albumin, *J. Mol. Struct.*, 970, 128-133 (2010).  
<https://doi.org/10.1016/j.molstruc.2010.02.061>

- Wang, H., Jiang, X., Zhou, I., Cheng, Z., Yin, W., Duan, M., Liu, P. and Jiang, X., Study of the interaction between 5-sulfosalicylic acid and bovine serum albumin by fluorescence spectroscopy, *J. Lumin.*, 134, 747-753 (2013).  
<https://doi.org/10.1016/j.jlumin.2012.06.053>
- Wu, F. Y., Ji, Z. J., Wu, Y. M., Wan, X. F., Interaction of ICT receptor with serum albumins in aqueous buffer, *Chem. Phys. Lett.*, 424, 387-393 (2006).  
<https://doi.org/10.1016/j.cplett.2006.05.019>
- Yuan, J. P., Guo, W. W., Yang, X. R., Wang, E. K., Anticancer drug-DNA interactions measured using a photoinduced electron-transfer mechanism based on luminescent quantum dots, *J. Anal. Chem.*, 81, 362-368 (2009).  
<https://doi.org/10.1021/ac801533u>
- Zhang, G., Wang, Y., Zhang, H., Tang, S. and Tao, W., Human serum albumin interaction with paraquat studied using spectroscopic methods, *Pestic. Biochem. Physiol.*, 87, 23-29 (2007).  
<https://doi.org/10.1016/j.pestbp.2006.05.003>
- Zhao, X., Liu, R., Chi, Z., Teng, Y. and Qin, P., New insights into the behavior of bovine serum albumin adsorbed onto carbon nanotubes: Comprehensive spectroscopic studies, *J. Phys. Chem. B*, 114, 5625-2631 (2010).  
<https://doi.org/10.1021/jp100903x>
- Zhou, N., Liang, Y. Z. and Wang, P., Characterization of the interaction between furosemide and bovine serum albumin, *J. Mol. Struct.*, 872, 190-196 (2008).  
<https://doi.org/10.1016/j.molstruc.2007.02.035>